

Supplemental materials for “ Li_3PO_4 electrolytes: Effects of O vacancies and N or Si substitutions on Li ion migration” by Y. A. Du and N. A. W. Holzwarth

Department of Physics, Wake Forest University, Winston-Salem, NC 27109.

August 9, 2008

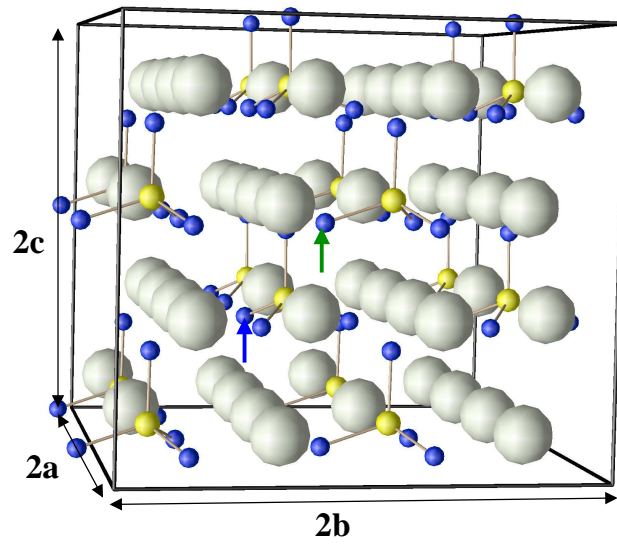
Defects based on the $\gamma\text{-Li}_3\text{PO}_4$ crystalline form are shown in Fig. 1 and 2 of the paper. We also constructed stable bent and straight PNP defects based on the $\beta\text{-Li}_3\text{PO}_4$ crystalline form as shown in Figs. 1 and 2 of this supplement.

In addition to the partial densities of states plots presented in the paper, we also examined the partial densities of states of several other configurations. Figure 3 compares the 4 different PNP structures studied. In addition to indicating the contribution from the bridging N sites, we also show that the partial densities of states of the “associated” O sites (those included in the $\text{O}_3\text{P-N-PO}_3$ unit) are well correlated with the contributions from the bridging N sites. It is very interesting to note that the 4 structures shown have very similar densities of states.

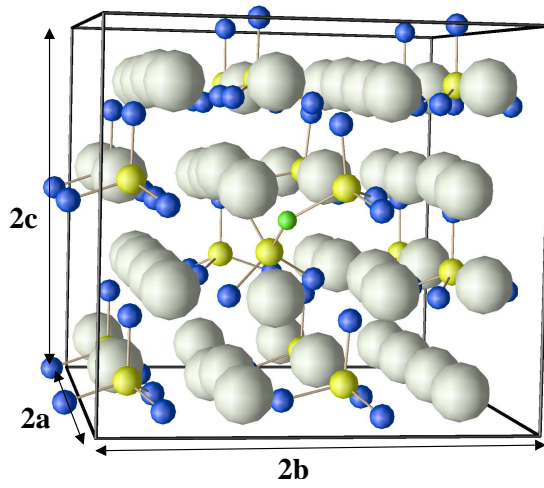
Figure 4 compares the partial densities of states of the 4 different POP structures studied. The initial configurations for these structures were taken from the corresponding supercells of the PNP structures by exchanging an O from a remote phosphate group with the N on the bridging site. In this case, the tetrahedral N contributions complicate the picture so are not included in the plot and the zero of energy is shifted accordingly. The bridging O contributions show a low energy $2p\sigma$ state below the bottom of the phosphate states, similar to the PNP case. More generally, the partial densities of states of both the bridging O sites and the “associated” O sites (those included in the $\text{O}_3\text{P-O-PO}_3$ unit) are lowered relative to those of the crystalline tetrahedral sites.

In order to further characterize the states associated with the straight P-N-P defect, we constructed contour plots for electron densities with energy ranges I-IV indicated in the densities of states plot shown in Fig. 5. The contour plots are shown in Fig. 6.

In order to further analyze the states associated with the PO_3N groups discussed in Sec. IV of the paper, we constructed contour plots for the electron densities associated with energy ranges I-V shown in the densities of states plot of Fig. 7 (slightly modified from Fig. 14 of the paper). The corresponding contour plots are given in Fig. 8.

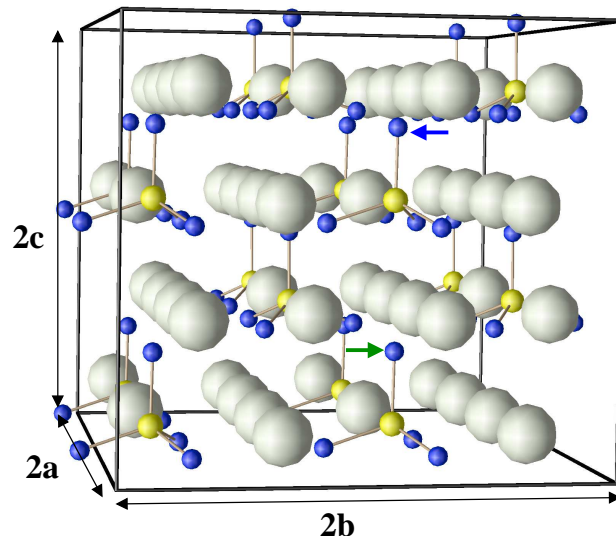


(a)

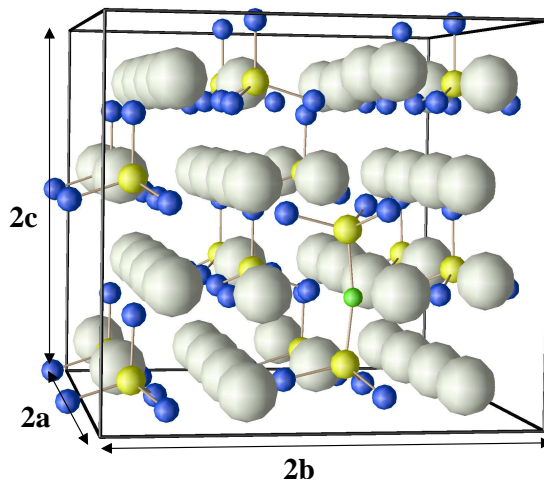


(b)

FIG. 1: Ball and stick diagram of β - Li_3PO_4 supercell indicating PO_4 groups with bonded yellow and blue spheres and Li ions with gray spheres. Diagram (a) shows the perfect crystal. Blue or green arrows indicate the sites where O will be removed or replaced with N, respectively, to form the relaxed “bent” PNP defect structure shown in (b), with the N site indicated with a green sphere.



(a)



(b)

FIG. 2: Similar diagrams to those in Fig. 1. The blue and green arrows in the perfect crystal diagram (a) indicate different O sites which result in the “straight” PNP defect structure shown in (b).

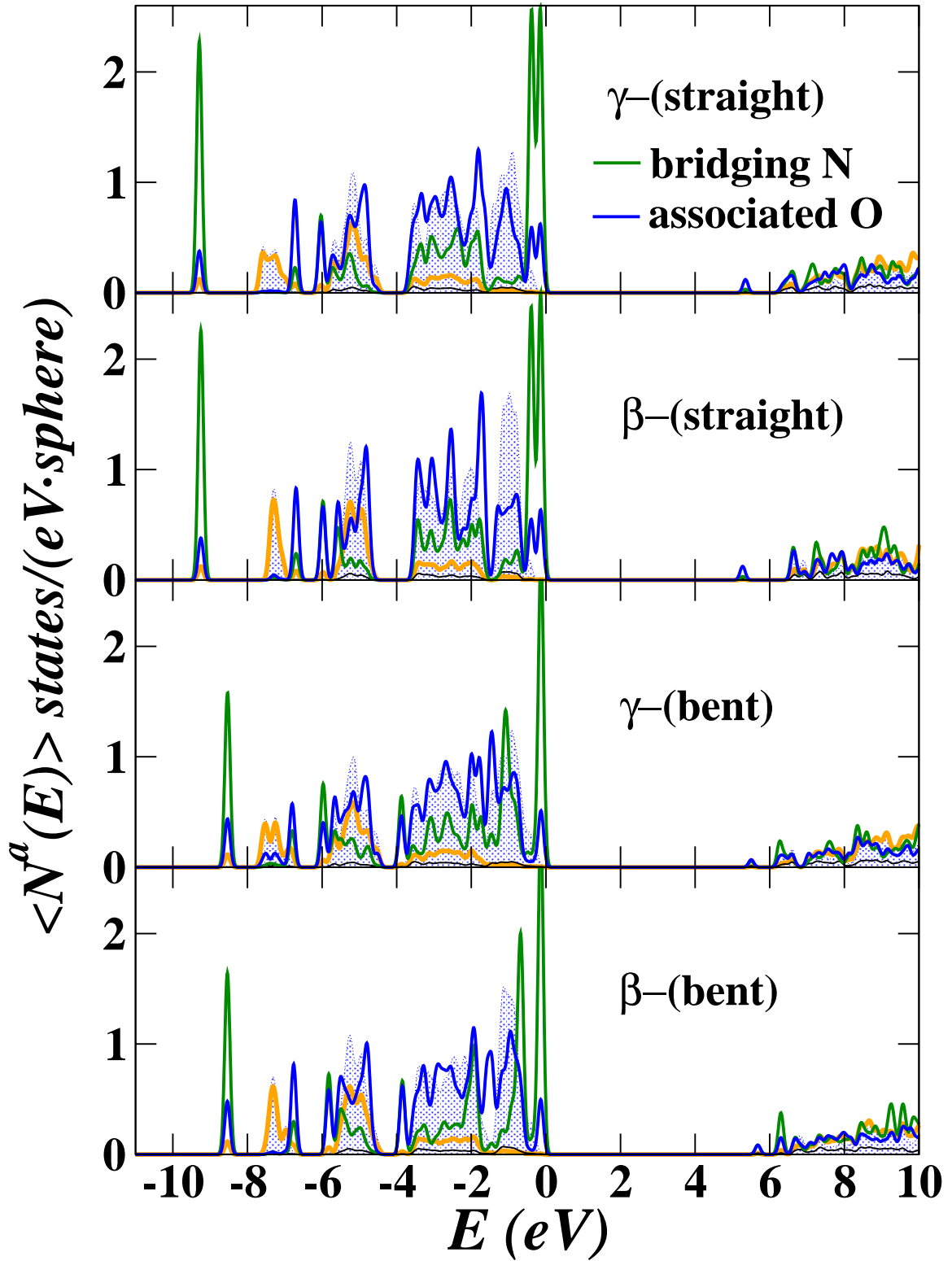


FIG. 3: Partial densities of states for $\text{Li}_{3-1/16}\text{PO}_{4-2/16}\text{N}_{1/16}$ including the $\text{O}_3\text{P}-\text{N}-\text{PO}_3$ defect, comparing bent and straight structures derived from the γ and β crystalline structures. The labels for the contributions from atoms not associated with the defect are the same as in Fig. 5 of the paper, while contributions from the bridging N sites and associated O sites are indicated with green and blue lines, respectively. The zero of energy is taken as the energy of the last occupied state.

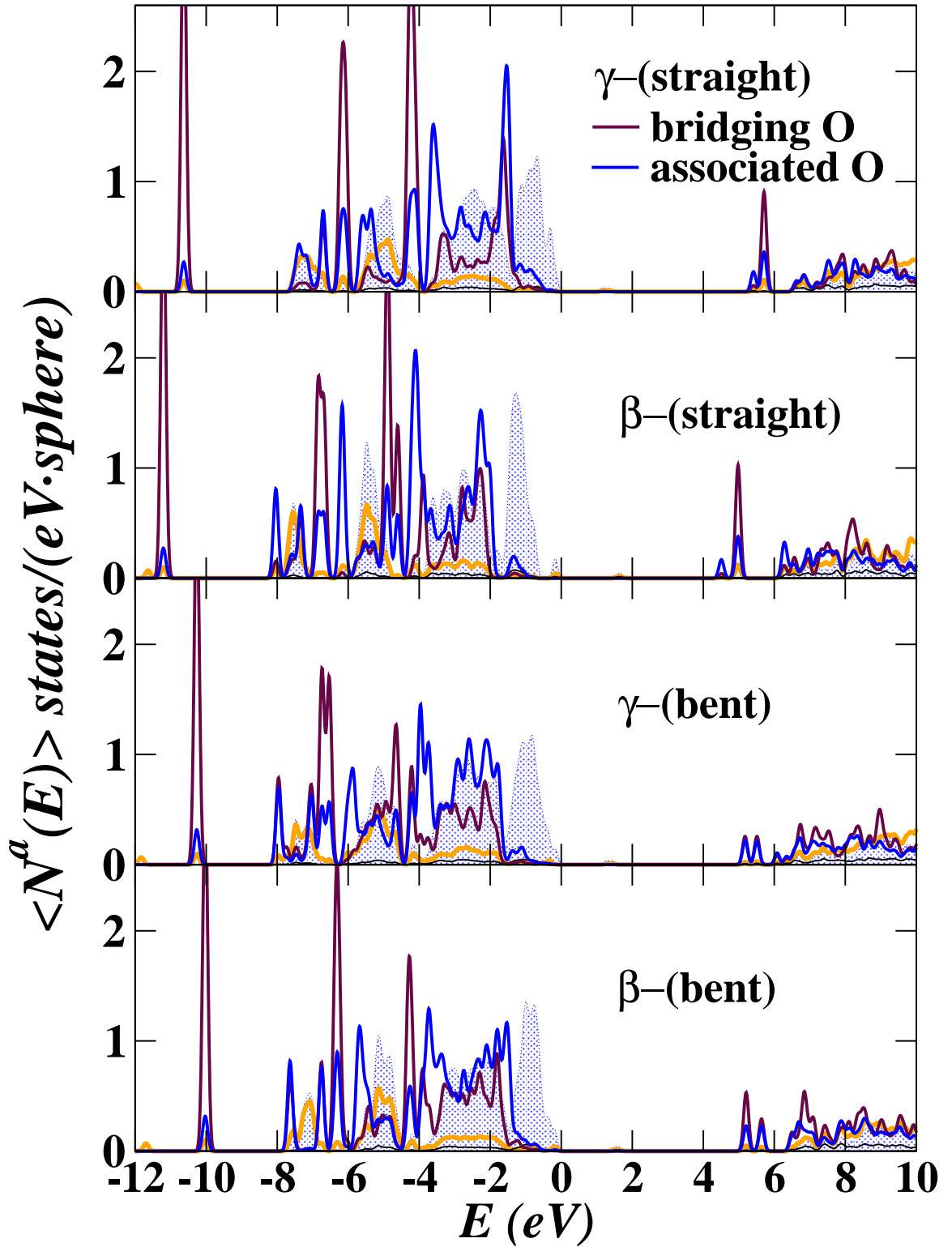


FIG. 4: Partial densities of states for $\text{Li}_{3-1/16}\text{PO}_{4-2/16}\text{N}_{1/16}$ including the $\text{O}_3\text{P}-\text{O}-\text{PO}_3$ defect and N replacing an O on a remote phosphate group. The N contributions are not shown in the figure and the zero of energy is adjusted to approximate the supercell without N. Bent and straight structures derived from the γ and β crystalline structures are compared, corresponding to the similar geometries of Fig. 3. The labels for the contributions from atoms not associated with the defect are the same as in Fig. 5 of the paper, while contributions from the bridging O sites and associated O sites are indicated with maroon and blue lines, respectively.

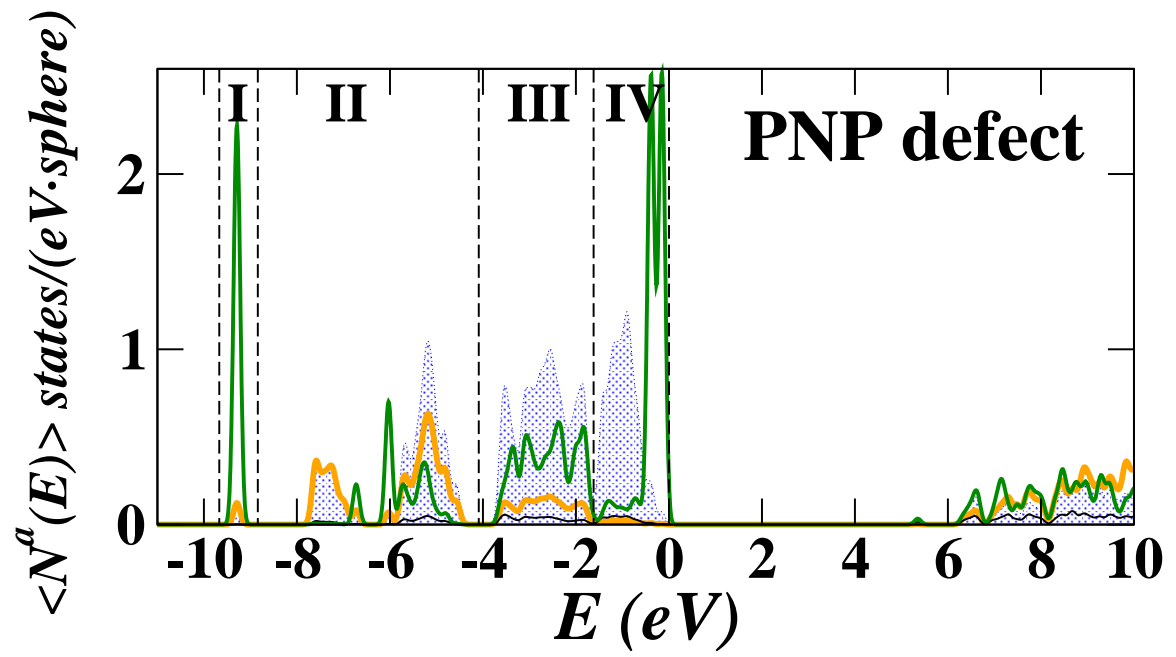


FIG. 5: Partial densities of states for the straight PNP structure in the $\text{Li}_{3-1/16}\text{PO}_{4-2/16}\text{N}_{1/16}$ supercell, showing energy regions for electron density plots shown in Fig. 6 below.

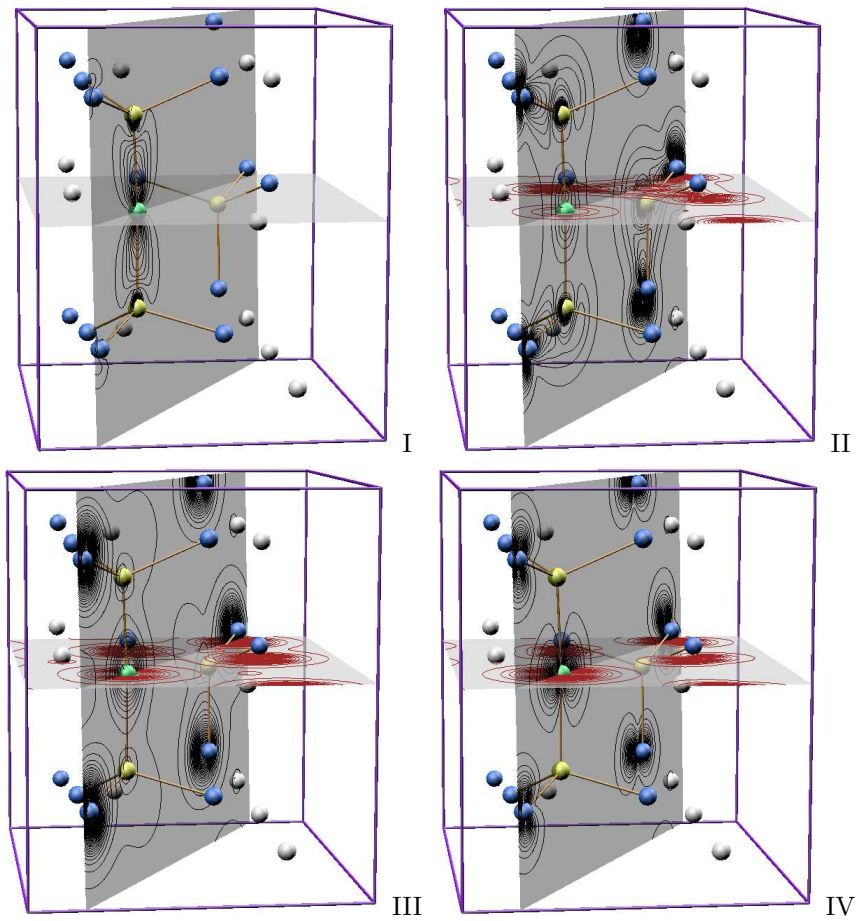


FIG. 6: Ball and stick model of “straight” P–N–P defect in the $\text{Li}_{3-1/16}\text{PO}_{4-2/16}\text{N}_{1/16}$ supercell showing superposed contours of electron density in the energy ranges indicated in Fig. 5. The P, O, N, and Li atoms are indicated with yellow, blue, green, and grey balls, respectively. The contours are given in intervals of $0.10 \text{ electrons}/\text{\AA}^3$ starting with the lowest contour of $0.05 \text{ electrons}/\text{\AA}^3$, in two different planes passing through the N site.

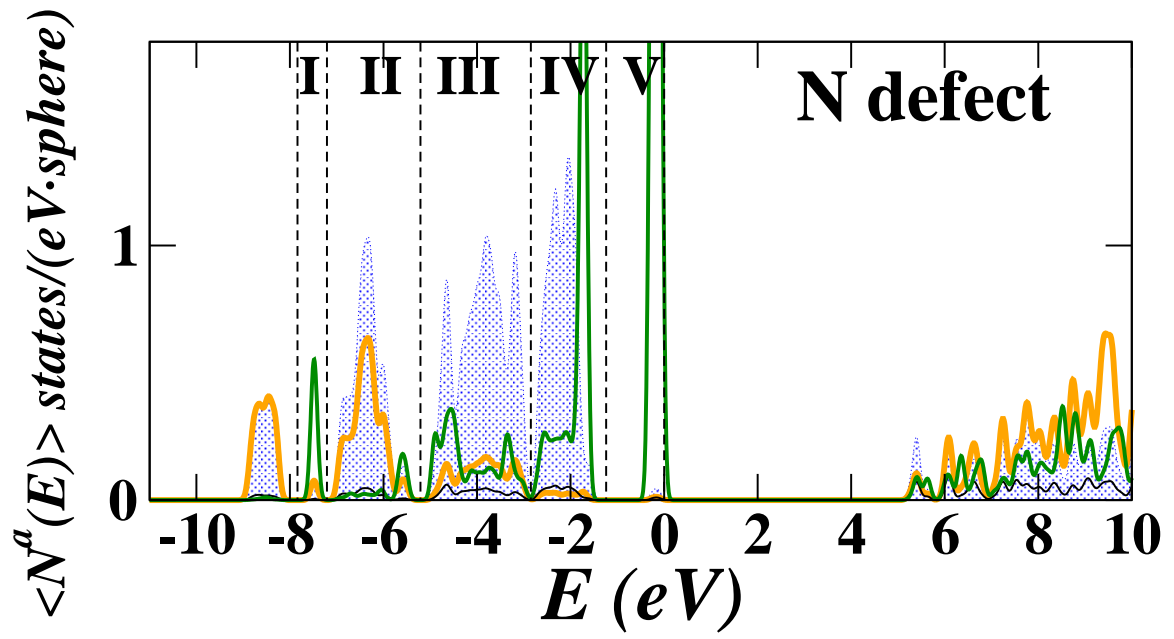


FIG. 7: Partial densities of states for the PO_3N defect in the $\text{Li}_{3+1/16}\text{PO}_{4-1/16}\text{N}_{1/16}$ supercell shown in Fig. 13 of the paper, similar to Fig. 14 of the paper, but showing energy regions for electron density plots shown in Fig. 8 below.

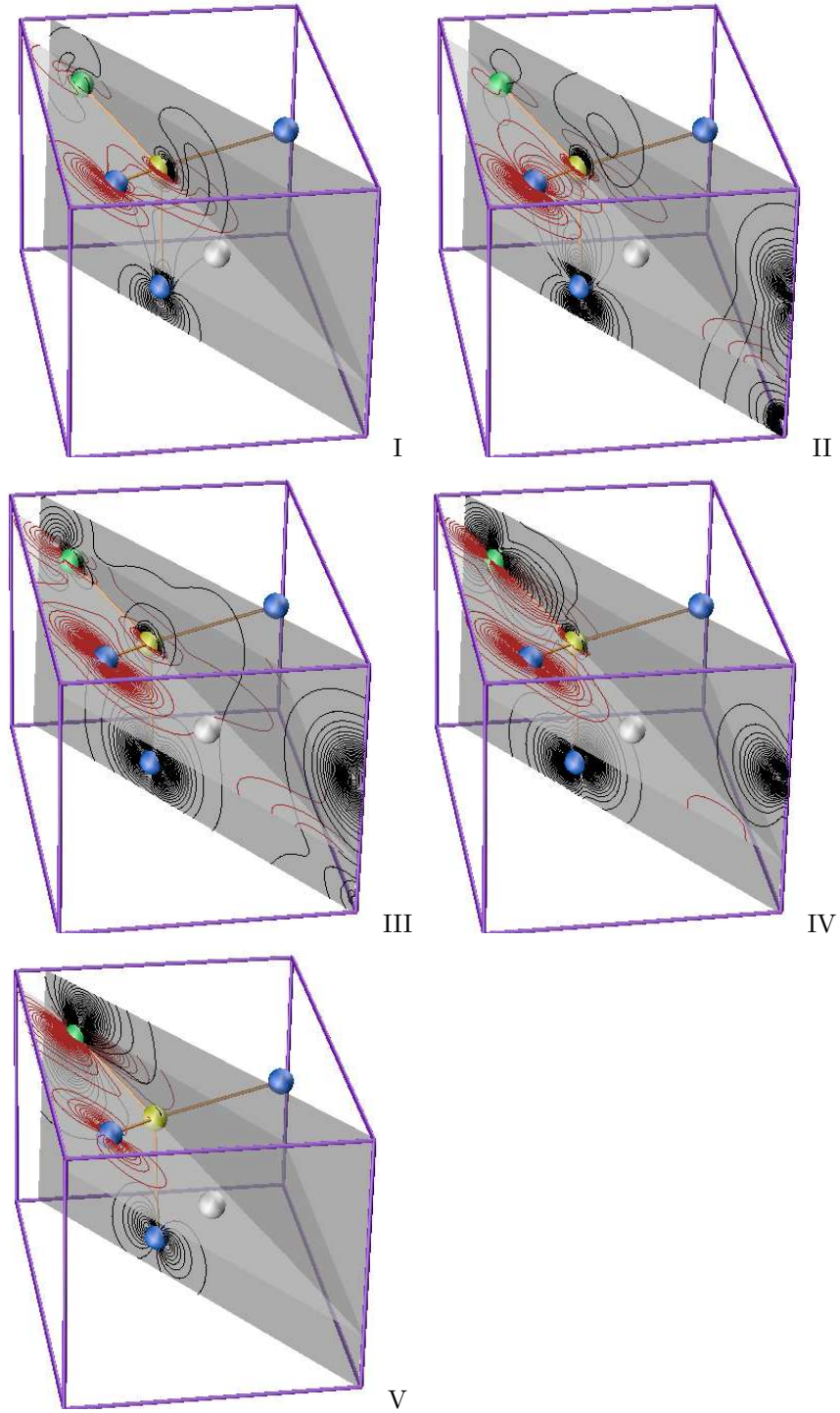


FIG. 8: Ball and stick model of PO_3N section of the $\text{Li}_{3+1/16}\text{PO}_{4-1/16}\text{N}_{1/16}$ supercell of Fig. 13 in the paper showing superposed contours of electron density in the energy ranges indicated in Fig. 7. The P, O, N, and Li atoms are indicated with yellow, blue, green, and grey balls, respectively. The contours are given in intervals of $0.10 \text{ electrons}/\text{\AA}^3$ starting with the lowest contour of $0.05 \text{ electrons}/\text{\AA}^3$, in two different planes passing through the N site.